Unitary Matrix Completion-Based DOA Estimation of Noncircular Signals in Nonuniform Noise

XIANPENG WANG[1], (Member, IEEE), **YANGHUI ZHU**[1], **MENGXING HUANG**[1],
JINGJING WANG[2], **LIANGTIAN WAN**[3], (Member, IEEE), **AND GUOAN BI**[4]

[1]State Key Laboratory of Marine Resource Utilization in South China Sea, College of Information and Communication Engineering, Hainan University, Haikou 570228, China
[2]College of Physics and Electronic Science, Shandong Normal University, Jinan 250014, China
[3]Key Laboratory for Ubiquitous Network and Service Software of Liaoning Province, School of Software, Dalian University of Technology, Dalian 116620, China
[4]School of Electrical and Electronic Engineering, Nanyang Technological University, Singapore 639798

Corresponding authors: Yanghui Zhu (zyhui1994@126.com) and Mengxing Huang (huangmx@163.com)

ABSTRACT In this paper, a novel direction-of-arrival (DOA) estimation algorithm is proposed for noncircular signals with nonuniform noise by using the unitary matrix completion (UMC) technique. First, the proposed method utilizes the noncircular property of signals to design a virtual array for approximately doubling the array aperture. Then, the virtual complex-valued covariance matrix with the unknown nonuniform noise is transformed into the real-valued one by utilizing the unitary transformation to improve the computational efficiency. Next, a novel UMC method is formulated for the DOA estimation to remove the influence of nonuniform noise. Finally, the DOA without the influence of the unknown noncircularity phase is obtained by using the modified estimation of signal parameters via rotational invariance technique (ESPRIT). Especially, for handling the coherent sources, the forward–backward spatial smoothing technique is utilized to reconstruct a full-rank covariance matrix so that the signal subspace and the noise subspace can be correctly separated. Due to utilizing the extended array aperture and the unitary transformation, the proposed method can identify more sources than the number of physical sensors and provides higher angular resolution and better estimation performance. Compared with the existing DOA estimation algorithms for noncircular signals, the proposed one can effectively suppress the influence of the nonuniform noise. The simulation results are provided to verify the effectiveness and superiority of the proposed method.

INDEX TERMS Direction-of-arrival estimation, noncircular, nonuniform noise, unitary matrix completion.

I. INTRODUCTION

Direction-of-arrival (DOA) estimation is an important research topic in the field of array signal processing, and has been widely applied to various scenarios, such as wireless communication, radar, sonar, navigation, seismic detection and medicine [1]. In the past decades, a large number of DOA estimation methods, such as multiple signal classification (MUSIC) [2], estimation of signal parameters via rotational invariance techniques (ESPRIT) [3] and maximum likelihood (ML) estimation [4], have been developed for

The associate editor coordinating the review of this manuscript and approving it for publication was Guan Gui.

improving the estimation performance. These methods are almost always applicable to multiple-input multiple-output (MIMO) radar systems [5], [6]. However, the majority of these methods assumed that sources are circular signals. The complex noncircular signal is often used in the real-valued modulation schemes, such as binary phase shift keying (BPSK), minimum shift keying (MSK) and unbalanced quaternary phase shift keyed (UQPSK), and these schemes have also been employed in most of modern applications, e.g., sonar, telecommunication and satellite systems. Unfortunately, these DOA estimation methods mentioned above have not utilized the noncircular property of the signal effectively.

So far, some subspace-based DOA estimation algorithms for noncircular signals have been proposed in [7]–[11]. In [7], the noncircular ESPRIT (NC-ESPRIT) method was proposed by exploiting noncircularity of signal to achieve the improved estimation performance and double the number of identifiable sources. However, it does not take account of coherent sources. By using the unitary transformation and the spatial smoothing technique, the NC unitary ESPRIT in [8] was proposed to improve computational efficiency and deal with coherent sources. As an extension of [7] and [8], the R-D NC unitary ESPRIT algorithm was proposed in [9], which can estimate the parameters of multidimensional (R-D) signal, and the spatially smoothed version of R-D NC unitary ESPRIT algorithm was proposed in [10]. However, the number of coherent sources estimated by these methods is limited. In [11], by designing a virtual center-symmetric array, the conjugate unitary ESPRIT (CU-ESPRIT) algorithm was proposed to estimate more coherent sources and further reduce the computational complexity. However, it requires noncircular signals to be real-valued, which is difficult to support practical systems. In addition, by utilizing the compressed sensing (CS) technology [12], [13], some sparse signal recovery (SSR)-based DOA estimation methods have been developed in [14]–[16]. By exploiting the block-sparse information, the nuclear norm minimization (NNM)-based methods have also been reported in [17], [18]. All of these methods have improved the estimation accuracy and angular resolution with the assumption that the noise is uniform white noise. However, when the noise becomes nonuniform, their estimated performance would deteriorate significantly due to the incorrect noise model.

The nonuniform noise can be regarded as the noise across the array is spatially white whereas the sensor noise variances are not identical. This model becomes relevant in situations with hardware nonideality in receiving channels as well as for sparse arrays with prevailing external noise such as reverberation noise in sonar or external seismic noise. Therefore, it is important to solve the nonuniform noise problem. In recent years, many feasible methods have been developed to solve DOA estimation with the unknown nonuniform noise [19]–[23]. In [21], two optimization problems based on the ML and least squares (LS) estimations are proposed by utilizing iterative method to estimate the signal and noise subspaces. However, it is time-consuming due to the iterative procedure. In order to eliminate the covariance matrix of nonuniform noise without using the iteration method, matrix completion technique was investigated in [22], which can transform the nonconvex problem into a convex one by using the nuclear norm minimization. However, its stability is poor. Similarly, another matrix completion method was proposed in [23], where the generalized least squares (GLS) sense and weighting matrix were analyzed. However, the above matrix completion-based methods generally require considerable computation because they deal with complex-valued covariance matrices. In order to improve the computational efficiency, the unitary transformation technique was introduced

in [24], [25]. The unitary transformation-based methods not only reduce the computational complexity, but also improve the estimation accuracy. Therefore, based on the advantages of the unitary transformation, we propose the unitary matrix completion method to suppress the influence of nonuniform noise.

In this paper, the unitary matrix completion framework for DOA estimation of noncircular signals is proposed. In the proposed method, by integrating the unitary matrix completion method and the modified CU-ESPRIT algorithm, the DOA of noncircular signal in nonuniform noise can be directly estimated. The main contributions of this paper are as follows

(a) The DOA estimation problem of noncircular signals under nonuniform noise is solved.

(b) The processing method of coherent noncircular signals under the above conditions is given.

(c) For an odd number of virtual arrays, new selection matrices are designed to estimate DOAs of noncircular signals.

In summary, the proposed method provides superior DOA estimation performance. Simulation results are provided to illustrate the performance of the proposed method.

This paper is organized as follows. The noncircular signal model impinging on ULA in the presence of unknown nonuniform noise is introduced in Section II. The design of the virtual array, the unitary transformation, the unitary matrix completion method and the forward-backward spatial smoothing technique are shown in Section III. The simulation results are presented and analyzed in Section IV. The conclusion is given in Section V.

Notation: $(\cdot)^T$, $(\cdot)^H$, $(\cdot)^*$, $Im(\cdot)$ and $Re(\cdot)$ denote transpose, conjugate-transpose, conjugate, imaginary part operator and real part operator, respectively. $\otimes$ and $\odot$ denote the Kronecker product and Khatri-Rao product, respectively. $\mathbf{I}_k$ denotes a $k \times k$ dimensional unit matrix, and $\mathbf{\Pi}_k$ denotes a $k \times k$ dimensional exchange matrix with ones on its anti-diagonal entries and zeros elsewhere. $\| \cdot \|_*$, $\| \cdot \|_2$ and $\| \cdot \|_F$ denote the nuclear norm, ℓ_2 norm and Frobenius norm, respectively. In addition, $diag\{\cdot\}$ denotes the diagonal matrix. $E\{\cdot\}$ and $rank\{\cdot\}$ denote the mathematical expectation and the rank of a matrix. $trace\{\cdot\}$ denotes the trace of a matrix and $vec(\cdot)$ denotes the vectorization operator.

II. SIGNAL MODEL

Consider a ULA with M sensors, and the adjacent sensor spacing, d, is set to be one-half of the wavelength, $\lambda/2$. It is assumed that the far-field noncircular narrow-band sources impinging on the array are from P distinct angular directions $\theta_1, \theta_2, \ldots, \theta_P$. The received data vector $\mathbf{x}(t) \in \mathbb{C}^{M \times 1}$ is expressed as [8]

$$\mathbf{x}(t) = \mathbf{A}\mathbf{s}(t) + \mathbf{n}(t) \qquad (1)$$

where the manifold matrix $\mathbf{A} = [\mathbf{a}(\theta_1), \mathbf{a}(\theta_2), \ldots, \mathbf{a}(\theta_P)] \in \mathbb{C}^{M \times P}$, and the manifold vector $\mathbf{a}(\theta_k) = [1, exp(j\pi sin\theta_k), \ldots, exp(j\pi(M-1)sin\theta_k)]^T$, and $\mathbf{s}(t) \in \mathbb{C}^{P \times 1}$ denotes the noncir-
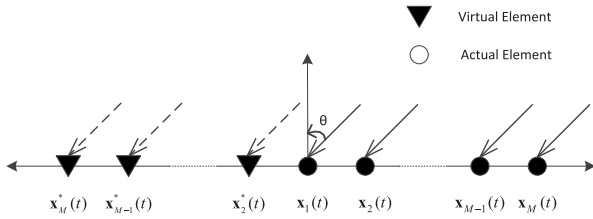
FIGURE 1. Illustration of the virtual array.

cular signal vector, which satisfies with

$$\mathbf{s}(t) = \mathbf{\Phi}\mathbf{s}_0(t) \qquad (2)$$

where $\mathbf{\Phi} = diag\{[exp(j\psi_1), \ldots, exp(j\psi_P)]\} \in \mathbb{C}^{P \times P}$ denotes a diagonal matrix containing the noncircularity phase $\boldsymbol{\psi} = [\psi_1, \ldots, \psi_P]$, which can be arbitrary for each signal, $\mathbf{s}_0(t) \in \mathbb{R}^{P \times 1}$ denotes the real-valued signal vector, and $\mathbf{n}(t) \in \mathbb{C}^{M \times 1}$ denotes the nonuniform Gaussian noise vector whose covariance matrix can be expressed as

$$\mathbf{Q} = E\{\mathbf{n}(t)\mathbf{n}^H(t)\} = diag\{\sigma_1^2, \sigma_2^2, \ldots, \sigma_M^2\} \qquad (3)$$

where σ_m^2 denotes the noise power from the mth sensor, and the noise powers of these sensors are assumed to be different and unknown. By collecting L snapshots, the received data in (1) can be rewritten as

$$\mathbf{X} = \mathbf{AS} + \mathbf{N} \qquad (4)$$

where $\mathbf{X} = [\mathbf{x}(t_1), \ldots, \mathbf{x}(t_L)] \in \mathbb{C}^{M \times L}$ denotes the received data matrix, $\mathbf{S} = \mathbf{\Phi}\mathbf{S}_0 \in \mathbb{C}^{P \times L}$ denotes the noncircular signal matrix with $\mathbf{S}_0 = [\mathbf{s}_0(t_1), \ldots, \mathbf{s}_0(t_L)] \in \mathbb{R}^{P \times L}$, and $\mathbf{N} = [\mathbf{n}(t_1), \ldots, \mathbf{n}(t_L)] \in \mathbb{C}^{M \times L}$ denotes the nonuniform Gaussian noise matrix.

III. UNITARY MATRIX COMPLETION FOR DOA ESTIMATION OF NONCIRCULAR SIGNALS
A. VIRTUAL ARRAY
Since noncircular signals have real components, their conjugation equals to themselves. By utilizing this property of noncircular signals, a virtual array is constructed as shown in Fig.1, which has $2M-1$ virtual array elements in total. The virtual array increases the number of array elements, which changes the signal model. Therefore, the observation vector $\mathbf{x}_v(t) \in \mathbb{C}^{(2M-1) \times 1}$ of the virtual array can be expressed as

$$\mathbf{x}_v(t) = [\mathbf{x}_M^*(t), \ldots, \mathbf{x}_2^*(t), \mathbf{x}_1(t), \mathbf{x}_2(t), \ldots, \mathbf{x}_M(t)]^T \qquad (5)$$

where $\mathbf{x}_i(t)$ denotes the data received by the ith sensor at the tth time instant. Therefore, the virtual array receiving data matrix is described as

$$\mathbf{X}_v = \begin{bmatrix} \mathbf{JX}^* \\ \mathbf{X} \end{bmatrix} = \begin{bmatrix} \mathbf{JA}^*\mathbf{S}^* \\ \mathbf{AS} \end{bmatrix} + \begin{bmatrix} \mathbf{JN}^* \\ \mathbf{N} \end{bmatrix} \qquad (6)$$

where $\mathbf{J} = [\mathbf{0}_{(M-1) \times 1} \mathbf{\Pi}_{M-1}]$. Because $\mathbf{S}_0 \in \mathbb{R}^{P \times L}$, we have $\mathbf{S}^* = \mathbf{\Phi}^*\mathbf{S}_0$. Therefore, (6) can be written as

$$\mathbf{X}_v = \begin{bmatrix} \mathbf{JA}^*\mathbf{\Phi}^* \\ \mathbf{A\Phi} \end{bmatrix} \mathbf{S}_0 + \begin{bmatrix} \mathbf{JN}^* \\ \mathbf{N} \end{bmatrix} = \mathbf{BS}_0 + \mathbf{N}_v \qquad (7)$$

where $\mathbf{B} = [\mathbf{b}(\theta_1, \psi_1), \ldots, \mathbf{b}(\theta_P, \psi_P)] \in \mathbb{C}^{(2M-1) \times P}$ denotes the virtual array manifold matrix, which contains noncircular phase, and the manifold vector $\mathbf{b}(\theta_i, \psi_i) \in \mathbb{C}^{(2M-1) \times 1}$ can be written as

$$\begin{aligned}\mathbf{b}(\theta_i, \psi_i) = [&exp(-j\pi(M-1)sin\theta_i)exp(-j\psi_i),\\ &\ldots, exp(-j\pi sin\theta_i)exp(-j\psi_i), 1\\ &\cdot exp(j\psi_i), exp(j\pi sin\theta_i)exp(j\psi_i),\\ &\ldots, exp(j\pi(M-1)sin\theta_i)exp(j\psi_i)]^T \quad (8)\end{aligned}$$

and $\mathbf{N}_v$ denotes the virtual array noise matrix.

Then the virtual array covariance matrix is obtained by

$$\mathbf{R}_v = E\{\mathbf{x}_v(t)\mathbf{x}_v^H(t)\} = \mathbf{R}_0 + \mathbf{Q}_v \qquad (9)$$

where $\mathbf{R}_0 = \mathbf{BPB}^H \in \mathbb{C}^{(2M-1) \times (2M-1)}$ denotes the virtual array noise-free covariance matrix, $\mathbf{P} = E\{\mathbf{s}_0(t)\mathbf{s}_0^H(t)\} \in \mathbb{R}^{P \times P}$ denotes the real-valued signal covariance matrix, and $\mathbf{Q}_v = diag\{\sigma_M^2, \ldots, \sigma_2^2, \sigma_1^2, \sigma_2^2, \ldots, \sigma_M^2\} \in \mathbb{R}^{(2M-1) \times (2M-1)}$ denotes the virtual array noise covariance matrix. In practice, the virtual array covariance matrix $\mathbf{R}_v$ is not available, and is estimated as

$$\hat{\mathbf{R}}_v = \frac{1}{L} \sum_{t=1}^{L} \mathbf{x}_v(t)\mathbf{x}_v^H(t). \qquad (10)$$

Obviously, when $\hat{\mathbf{R}}_v$ is adopted instead, we have $\hat{\mathbf{R}}_v \neq \mathbf{R}_0 + \mathbf{Q}_v$. Because this estimation error cannot be ignored, it will be discussed in a GLS sense below.

B. UNITARY TRANSFORMATION
Before discussing this estimation error, let's preprocess the estimated virtual array covariance matrix. It is well known that the complex-valued matrix operations are often used in most DOA estimation algorithms. By exploiting the unitary transformation, the complex-valued matrix can be transformed into a real-valued one, which reduces the computational complexity significantly. In addition, it has been proved in [25] that the DOA estimation performance can be improved by utilizing the real-valued structure. These merits motivate us to convert the complex-valued covariance matrix into real-valued one for DOA estimation.

By exploiting the center-Hermitian property of the virtual array covariance matrix $\mathbf{R}_v$, the real-valued one is derived as [11]

$$\mathbf{C}_v = \mathbf{U}_{2M-1}^H \mathbf{R}_v \mathbf{U}_{2M-1} \qquad (11)$$

where $\mathbf{C}_v$ denotes the virtual array real-valued covariance matrix and the odd-order unitary matrix $\mathbf{U}_{2n-1}$ is defined as

$$\mathbf{U}_{2n-1} = \frac{1}{\sqrt{2}} \begin{bmatrix} \mathbf{I}_{n-1} & \mathbf{0}_{(n-1) \times 1} & j\mathbf{I}_{n-1} \\ \mathbf{0}_{(n-1) \times 1}^T & \sqrt{2} & \mathbf{0}_{(n-1) \times 1}^T \\ \mathbf{\Pi}_{n-1} & \mathbf{0}_{(n-1) \times 1} & -j\mathbf{\Pi}_{n-1} \end{bmatrix}. \qquad (12)$$

However, in practice, because $\hat{\mathbf{R}}_v$ is not exactly center-Hermitian matrix, (11) is unavailable directly. Fortunately,
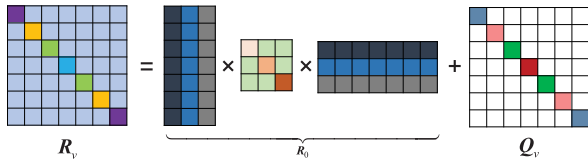
FIGURE 2. Illustration of the virtual array covariance matrix.

it has been proven in [24] that this problem can be solved by

$$\hat{\mathbf{C}}_v = Re\{\mathbf{U}_{2M-1}^H \hat{\mathbf{R}}_v \mathbf{U}_{2M-1}\} \quad (13)$$

where $\hat{\mathbf{C}}_v$ denotes the estimated real-valued virtual array covariance matrix.

C. UNITARY MATRIX COMPLETION

Matrix completion technique is an efficient method to recover a low-rank matrix by observing some elements of the matrix. The virtual array covariance matrix structure is shown in Fig.2. From (9), it is obvious that the virtual array noise-free covariance matrix $\mathbf{R}_0$ is a low rank matrix and the unknown nonuniform virtual array noise covariance matrix $\mathbf{Q}_v$ only affects the diagonal elements of the virtual array covariance matrix $\mathbf{R}_v$. If $\mathbf{R}_v$ is known, then $\mathbf{R}_0$ can be almost known except for its diagonal entries. Hence, by removing the diagonal elements of $\mathbf{R}_v$ and recovering the entire $\mathbf{R}_0$, the estimation problem of $\mathbf{R}_0$ can be solved, which can be regarded as a matrix completion problem. Once $\mathbf{R}_0$ is determined, the subspace-based algorithms can be applied to estimate the DOA without being affected by nonuniform noise. In the following, we introduce the unitary matrix completion method.

In order to reduce the computational complexity, (9) is substituted into (11) to yield

$$\mathbf{C}_v = \mathbf{U}_{2M-1}^H (\mathbf{R}_0 + \mathbf{Q}_v)\mathbf{U}_{2M-1} = \mathbf{R}_t + \mathbf{Q}_t \quad (14)$$

where $\mathbf{R}_t = \mathbf{U}_{2M-1}^H \mathbf{R}_0 \mathbf{U}_{2M-1} \in \mathbb{R}^{(2M-1)\times(2M-1)}$ denotes the virtual array real-valued noise-free covariance matrix, and $\mathbf{Q}_t = \mathbf{U}_{2M-1}^H \mathbf{Q}_v \mathbf{U}_{2M-1} \in \mathbb{R}^{(2M-1)\times(2M-1)}$ denotes the virtual noise matrix. It is worth mentioning that $\mathbf{R}_t$ and $\mathbf{Q}_t$ contain the characteristics of $\mathbf{R}_0$ and $\mathbf{Q}_v$, respectively. Because $\mathbf{R}_t$ is the real-valued form of $\mathbf{R}_0$ by using unitary transformation, it is a low-rank matrix. In addition, $\mathbf{Q}_t$ is a diagonal matrix whose diagonal elements are not completely the same. In other words, $\mathbf{R}_t$ and $\mathbf{Q}_t$ also conform to the analysis of the above matrix completion technique. Therefore, $\mathbf{R}_t$ can be determined by solving the following rank minimum problem

$$\underset{\mathbf{R}_t}{minimize}\ rank(\mathbf{R}_t)$$
$$subject\ to\ \mathcal{P}_\Omega(\mathbf{R}_t) = \mathcal{P}_\Omega(\mathbf{C}_v) \quad (15)$$

where $\mathcal{P}_\Omega : \mathbb{C}^{(2M-1)\times(2M-1)} \rightarrow \mathbb{C}^{(2M-1)\times(2M-1)}$ denotes a sampling operator, defined as

$$[\mathcal{P}_\Omega(\mathbf{X})]_{ij} = \begin{cases} \mathbf{X}_{ij}, & i \neq j \\ 0, & otherwise \end{cases} \quad (16)$$

where $[\mathcal{P}_\Omega(\mathbf{X})]_{ij}$ and $\mathbf{X}_{ij}$ denote the (i,j)th entry of $\mathcal{P}_\Omega(\mathbf{X})$ and $\mathbf{X}$, respectively.

Because the optimization problem of (15) is NP-hard, it is not solvable in polynomial time deterministically. As the tightest convex relation of the rank minimization, the nuclear norm minimization is often used to solve this optimization problem as follows

$$\underset{\mathbf{R}_t}{minimize}\ ||\mathbf{R}_t||_*$$
$$subject\ to\ \mathcal{P}_\Omega(\mathbf{R}_t) = \mathcal{P}_\Omega(\mathbf{C}_v). \quad (17)$$

Since $\mathbf{R}_t$ is a positive-semidefinite Hermitian matrix, we have $||\mathbf{R}_t||_* = trace\{\mathbf{R}_t\}$. Moreover, the constraint in (17) can be modified as $\mathbf{C}_v = \mathbf{R}_t + \mathbf{Q}_t, \mathbf{R}_t \succeq 0, \mathbf{Q}_t \in \mathcal{D}^+$, where $\succeq \mathbf{0}$ denotes the matrix is the positive-semidefinite Hermitian matrix, and $\mathcal{D}^+$ denotes the real-valued diagonal matrix. Therefore, we have

$$\underset{\mathbf{R}_t,\mathbf{Q}_t}{minimize}\ trace\{\mathbf{R}_t\}$$
$$subject\ to\ \mathbf{C}_v = \mathbf{R}_t + \mathbf{Q}_t, \quad \mathbf{R}_t \succeq 0,\ \mathbf{Q}_t \in \mathcal{D}^+. \quad (18)$$

Because only the estimated virtual array real-valued covariance matrix $\hat{\mathbf{C}}_v$ in (13) is available, the above constraint cannot be used in practice. Fortunately, this problem can be solved in a GLS sense.

The estimation error of the virtual array covariance vector and real-valued covariance vector are defined as $\boldsymbol{\xi} = vec(\hat{\mathbf{R}}_v - \mathbf{R}_v)$ and $\boldsymbol{\xi}_T = vec(\hat{\mathbf{C}}_v - \mathbf{C}_v)$, respectively. According to [26], $\boldsymbol{\xi}$ obeys complex Gaussian distribution $\boldsymbol{\xi} \sim \mathcal{CN}(0, \mathbf{W})$, and $\boldsymbol{\xi}_T$ obeys Gaussian distribution $\boldsymbol{\xi}_T \sim \mathcal{N}(0, \mathbf{C})$, where $\mathbf{W} = \frac{1}{L}(\mathbf{R}_v^T \otimes \mathbf{R}_v)$, $\mathbf{C} = \frac{1}{2}Re\{\mathbf{F}\mathbf{W}\mathbf{F}^H\}$, and $\mathbf{F} = \mathbf{U}_{2M-1}^T \otimes \mathbf{U}_{2M-1}^H$. Therefore, in a GLS sense, and considering $\hat{\mathbf{C}}_v$, the problem in (18) can be reformulated as [23]

$$\underset{\mathbf{R}_t,\mathbf{Q}_t}{minimize}\ trace\{\mathbf{R}_t\}$$
$$subject\ to\ ||\mathbf{C}^{-\frac{1}{2}}vec(\hat{\mathbf{C}}_v - \mathbf{R}_t - \mathbf{Q}_t)||_2^2 \leq \varepsilon$$
$$\mathbf{R}_t \succeq \mathbf{0}, \quad \mathbf{Q}_t \in \mathcal{D}^+ \quad (19)$$

where ε is a user-defined parameter. The estimation problem of the virtual array real-valued noise-free covariance matrix with the influence of nonuniform noise is solved in (19). However, in practice, the covariance matrix $\mathbf{C}$ should be estimated based on $\hat{\mathbf{C}} \triangleq \frac{1}{2}Re\{\mathbf{F}\hat{\mathbf{W}}\mathbf{F}^H\}$, where $\hat{\mathbf{W}} = \frac{1}{L}(\hat{\mathbf{R}}_v^T \otimes \hat{\mathbf{R}}_v)$. Thus, the noise-free and noise covariance matrices are estimated by solving the following convex problem

$$\underset{\mathbf{R}_t,\mathbf{Q}_t}{minimize}\ trace\{\mathbf{R}_t\}$$
$$subject\ to\ ||\hat{\mathbf{C}}^{-\frac{1}{2}}vec(\hat{\mathbf{C}}_v - \mathbf{R}_t - \mathbf{Q}_t)||_2^2 \leq \varepsilon$$
$$\mathbf{R}_t \succeq 0, \quad \mathbf{Q}_t \in \mathcal{D}^+. \quad (20)$$

The above method is called unitary matrix completion (UMC) method, and (20) can be solved efficiently by utilizing an optimization toolbox [27].

D. DOA ESTIMATION

The real-valued noise-free covariance matrix $\hat{\mathbf{R}}_t$ can be recovered in (20). Then the DOAs can be determined by using the unitary subspace-based algorithms. It is worth mentioning that the CU-ESPRIT algorithm in [11] needs to preprocess for noncircular signals, i.e., calculating and compensating their phases, which seriously affects the practicability of the algorithm. If the CU-ESPRIT algorithm is used, the estimated direction becomes biased due to the noncircular phase. This shortcoming motivates us to modify the CU-ESPRIT algorithm to directly estimate DOAs of noncircular signals. Our modify strategy is to design some novel selection matrices of CU-ESPRIT algorithm.

According to [11], the DOA estimation of noncircular signals can be obtained by solving

$$\mathbf{H}_{v1}\mathbf{E}_s\mathbf{\Psi} = \mathbf{H}_{v2}\mathbf{E}_s \tag{21}$$

where $\mathbf{E}_s$ is composed of the eigenvectors corresponding to the first P largest eigenvalues of $\hat{\mathbf{R}}_t$, and $\mathbf{H}_{v1}$ and $\mathbf{H}_{v2}$ are defined as

$$\mathbf{H}_{v1} = Re\{\mathbf{U}_{2M-1}^H\mathbf{J}_{v1}\mathbf{U}_{2M-1}\}, \tag{22}$$
$$\mathbf{H}_{v2} = Im\{\mathbf{U}_{2M-1}^H\mathbf{J}_{v2}\mathbf{U}_{2M-1}\} \tag{23}$$

where $\mathbf{J}_{v1}$ and $\mathbf{J}_{v2}$ are selection matrices. Considering the noncircular phase, we use the selection matrices defined in [8]. However, they only apply to $\mathbf{E}_s$ with an even number of rows. For $\mathbf{E}_s$ with an odd number of rows, we need to modify them simply, i.e., ignoring the data in the middle row of $\mathbf{E}_s$. Even if some data is lost, it has little effect on the DOA estimation results. Thus, the modified selection matrix can be obtained by (24) and (25), shown at the bottom of the next page.

Then, the eigenvalues $\omega_k (k = 1, \ldots, P)$ of $\mathbf{\Psi}$ are computed. Finally, the DOAs of noncircular signals can be expressed as

$$\theta_k = arcsin(-\frac{\lambda}{\pi d}arctan(\omega_k)). \tag{26}$$

The above modified CU-ESPRIT algorithm can directly estimate DOAs of noncircular signals, which is referred to as the MCU-ESPRIT algorithm.

E. FORWARD-BACKWARD SPATIAL SMOOTHING

The above analysis assumes that sources are uncorrelated. However, coherent sources often exist. In this case, the performance of many high-resolution DOA estimation algorithms would suffer from significant degradation. Because coherent sources make the rank defect of array covariance matrix, signal and noise subspaces cannot be distinguished correctly, which leads to the failure of subspace-based DOA estimation algorithm. The forward-backward spatial smoothing technique is often used to solve coherent signals in subspace-based algorithms. To separate coherent noncircular sources, the virtual subarrays were proposed in [11], [28] by using the spatial smoothing techniques. However, they

assume that sources are real-valued, i.e., the phase of the noncircular signal is $\psi_i = 0$ for an ideal case. This shortcoming motivates us to propose a method to solve the DOA estimation problem of coherent noncircular signals.

Let us first divide the virtual array into $K = (2M - 1) - \tilde{M} + 1$ overlapping virtual subarrays, each of which has $\tilde{M}$ virtual sensor elements. It has been proved in [29] that the modified covariance matrix of signals is a full rank matrix when the number of subarrays is larger than or equal to the number of signals, i.e., $K \geq P$. In addition, it requires that the size of each subarray must be at least $P + 1$. Considering that the number of coherent sources is at least two and the virtual array is a central-symmetric array, each virtual subarray is required to contain three or more actual elements. Therefore, similar to the forward-backward spatial smoothing algorithm in [30], the derivation detail is shown below.

For forward spatial smoothing, the kth virtual subarray covariance matrix can be expressed as $\mathbf{R}_k^f \in \mathbb{C}^{\tilde{M} \times \tilde{M}}$ to denote the diagonal part of $\mathbf{R}_v$. Then we have $\mathbf{R}_s^f = \frac{1}{K}\sum_{k=1}^{K}\mathbf{R}_k^f$, where $\mathbf{R}_s^f \in \mathbb{C}^{\tilde{M} \times \tilde{M}}$ denotes the forward spatial smoothed covariance matrix. For backward spatial smoothing, the kth virtual subarray covariance matrix can be expressed as $\mathbf{R}_k^b \in \mathbb{C}^{\tilde{M} \times \tilde{M}}$ to denote the diagonal part of $\mathbf{\Pi}_{\tilde{M}}\mathbf{R}_v^*\mathbf{\Pi}_{\tilde{M}}$. Then we have $\mathbf{R}_s^b = \frac{1}{K}\sum_{k=1}^{K}\mathbf{R}_k^b$, where $\mathbf{R}_s^b \in \mathbb{C}^{\tilde{M} \times \tilde{M}}$ denotes the backward spatial smoothed covariance matrix. Therefore, the virtual array forward-backward spatial smoothed covariance matrix $\mathbf{R}_s^{fb} \in \mathbb{C}^{\tilde{M} \times \tilde{M}}$ can be obtained as

$$\mathbf{R}_s^{fb} = \frac{1}{2}(\mathbf{R}_s^f + \mathbf{R}_s^b). \tag{27}$$

By exploiting unitary transformation, the estimated smoothed virtual array real-valued covariance matrix $\hat{\mathbf{C}}_s$ is derived as

$$\hat{\mathbf{C}}_s = Re\{\mathbf{U}_{\tilde{M}}^H\hat{\mathbf{R}}_s^{fb}\mathbf{U}_{\tilde{M}}\} \tag{28}$$

where $\hat{\mathbf{R}}_s^{fb}$ denotes the estimation matrix of $\mathbf{R}_s^{fb}$. It is worth mentioning that $\hat{\mathbf{C}}_v$ and $\hat{\mathbf{C}}_s$ have the same properties, and their noise components can be removed by using the unitary matrix completion method. Finally, besides using different selection matrices, the DOA estimation method of coherent signals is the same as that of uncorrelated signals. Similarly, the selection matrices of coherent sources are defined as

$$\mathbf{J}_{s1} = \begin{bmatrix} \mathbf{I}_{M-K-1} & \mathbf{0}_{(M-K-1)\times 1} & \mathbf{0}_{(M-K-1)\times M} \\ \mathbf{0}_{(M-K-1)\times M} & \mathbf{I}_{M-K-1} & \mathbf{0}_{(M-K-1)\times 1} \end{bmatrix}, \tag{29}$$

$$\mathbf{J}_{s2} = \begin{bmatrix} \mathbf{0}_{(M-K-1)\times 1} & \mathbf{I}_{M-K-1} & \mathbf{0}_{(M-K-1)\times M} \\ \mathbf{0}_{(M-K-1)\times M} & \mathbf{0}_{(M-K-1)\times 1} & \mathbf{I}_{M-K-1} \end{bmatrix}. \tag{30}$$

F. SUMMARY AND CRAMER-RAO BOUND

For uncorrelated sources, the procedure of the proposed method is summarized in Algorithm 1. For coherent sources, the procedure of the proposed method is summarized in Algorithm 2.

Algorithm 1 UMC for DOA Estimation of Uncorrelated Noncircular Signals in the Presence of Nonuniform Noise

---
1: Construct the virtual array receiving data matrix $\mathbf{X}_v$ using (6), and compute the estimated virtual array covariance matrix $\hat{\mathbf{R}}_v$ using (10).
2: Obtain the estimated real-valued virtual array covariance matrix $\hat{\mathbf{C}}_v$ using (13).
3: Recover the estimated real-valued virtual array noise-free covariance matrix $\hat{\mathbf{R}}_t$ using (20).
4: Perform the EVD of $\hat{\mathbf{R}}_t$ and return $\hat{\mathbf{E}}_s$.
5: Estimate the DOA using (26).

Algorithm 2 UMC for DOA Estimation of Coherent Noncircular Signals in the Presence of Nonuniform Noise

---
1: Construct the virtual array receiving data matrix $\mathbf{X}_v$ using (6), and compute the estimated virtual array covariance matrix $\hat{\mathbf{R}}_v$ using (10).
2: Compute the estimated virtual array forward-backward spatial smoothed covariance matrix $\hat{\mathbf{R}}_s^{fb}$.
3: Obtain the estimated virtual array forward-backward spatial smoothed real-valued covariance matrix $\hat{\mathbf{C}}_s$ using (28).
4: Recover the estimated real-valued virtual array noise-free covariance matrix $\hat{\mathbf{R}}_t$ using (20).
5: Perform the EVD of $\hat{\mathbf{R}}_t$ and return $\hat{\mathbf{E}}_s$.
6: Estimate the DOA using (29), (30) and (26).

Remark 1: It is noteworthy that due to the influence of noncircular phase, the spatial smoothing process will destroy the special structure of sources. If the virtual subarrays method proposed in [11] is adopted to solve the coherent source problem, the special structure of the source will be completely destroyed, resulting in the failure of DOA estimation. Because the proposed method requires each virtual subarray to contain at least three actual elements, the special structure of the source is not completely destroyed. Therefore, these selection matrices in (29) and (30) are to select the sources that have not been destroyed for DOA estimation. Nevertheless, since the proposed method uses the spatial smoothing technique, its performance inevitably decreases.

Remark 2: Considering that the virtual subarray contains at least three actual elements, the proposed method can estimate at most $M - 2$ coherent sources. Nevertheless, the proposed method can estimate more coherent sources than the unitary ESPRIT algorithm in [25] and the NC unitary ESPRIT algorithm in [8].

Remark 3: From the previous discussions, it is obvious that the proposed method has certain computational complexity for using the extension of the array aperture. First, computing $\hat{\mathbf{R}}_v$ in (10) requires $O\{(2M - 1)^2 L\}$. Compared with the subsequent convex optimization process, the computational complexity of the unitary transformation process is very low and can be ignored. Then, computing $\hat{\mathbf{W}} = \frac{1}{L}(\hat{\mathbf{R}}_v^T \otimes \hat{\mathbf{R}}_v)$ and $\hat{\mathbf{C}} \triangleq \frac{1}{2}Re\{\mathbf{F}\hat{\mathbf{W}}\mathbf{F}^H\}$ requires $O\{(2M - 1)^4\}$, where the computational complexity of $\hat{\mathbf{C}} \triangleq \frac{1}{2}Re\{\mathbf{F}\hat{\mathbf{W}}\mathbf{F}^H\}$ is ignored due to its low computational complexity. Next, solving the convex optimization problem in (20) requires $O\{\frac{1}{4}(2M - 1)^6\}$, where all calculations are real-valued. Finally, since $\hat{\mathbf{R}}_t$ is a real-valued positive-semidefinite Hermitian matrix, the EVD of $\hat{\mathbf{R}}_t$ is also real-valued, so that it only requires $O\{\frac{1}{4}(2M - 1)^3\}$. In summary, the proposed method with uncorrelated sources requires $O\{(2M - 1)^2 L + (2M - 1)^4 + \frac{1}{4}(2M - 1)^6 + \frac{1}{4}(2M - 1)^3\}$. However, combining the ESPRIT algorithm in [3] with the LRMD method in [23], the method only requires $O\{M^2 L + M^4 + M^6 + M^3\}$.

Cramér-Rao Bound (CRB): According to [31], the CRB based on the received data of noncircular signals in nonuniform noise can be expressed as

$$\text{CRB} = \{\bar{\mathbf{F}}_1 - \bar{\mathbf{F}}_2\bar{\mathbf{F}}_3^{-1}\bar{\mathbf{F}}_4\}^{-1} \tag{31}$$

where $\bar{\mathbf{F}}_1 = L\mathbf{D}_1^H\mathbf{W}_R\mathbf{D}_1, \bar{\mathbf{F}}_2 = L\mathbf{D}_1^H\mathbf{W}_R\mathbf{D}_2$, $\bar{\mathbf{F}}_3 = L\mathbf{D}_2^H\mathbf{W}_R\mathbf{D}_2$, $\bar{\mathbf{F}}_4 = L\mathbf{D}_2^H\mathbf{W}_R\mathbf{D}_1$, $\mathbf{W}_R = \mathbf{R}_v^{-T} \otimes \mathbf{R}_v^{-1}$, $\mathbf{D}_1 = [\bar{\mathbf{A}}^*\mathbf{\Phi}^* \odot \bar{\mathbf{A}}'\mathbf{\Phi} + (\bar{\mathbf{A}}')^*\mathbf{\Phi}^* \odot \bar{\mathbf{A}}\mathbf{\Phi}]\mathbf{P}$, $\bar{\mathbf{A}} = \begin{bmatrix} \mathbf{J}\mathbf{A}^* \\ \mathbf{A} \end{bmatrix}$, $\bar{\mathbf{A}}' = [\partial\bar{\mathbf{a}}(\theta_1)/\partial(\theta_1), \ldots, \partial\ \bar{\mathbf{a}}(\theta_P)/\partial(\theta_P)]$, $\bar{\mathbf{a}}(\theta_k) = [exp(-j\pi(M - 1)sin\theta_k), \ldots, 1, \ldots, exp(j\pi(M - 1)sin\theta_k)]$ and $\mathbf{D}_2 = [\bar{\mathbf{A}}^*\mathbf{\Phi}^* \odot \mathbf{A}\mathbf{\Phi}, \mathbf{I}_{2M-1} \odot \mathbf{I}_{2M-1}]$.

IV. SIMULATION RESULTS
In this section, some simulation results are presented to illustrate the performance of the proposed method by comparing it with other methods, which include the MCU-ESPRIT method and the LRMD method in [23]. Among them, the MCU-ESPRIT method is a modified version of the CU-ESPRIT method in [11], which can estimate the DOAs of noncircular signals, and the LRMD method uses traditional ESPRIT algorithm to obtain DOAs. In our simulations, a ULA has $M = 8$ sensors, and the adjacent sensor spacing is one-half wavelength. It is assumed that sources are narrow-band noncircular signals (BPSK, UQPSK or MSK modulation), and the powers of source signals are the same, which can be expressed as σ_s^2. The noise, $\boldsymbol{\sigma} = [\sigma_1^2, \sigma_2^2, \ldots, \sigma_M^2]^T$, is nonuniform, and their powers are not exactly equal to each other. The signal-to-noise ratio (SNR) is defined as SNR$= \frac{1}{M}\Sigma_{m=1}^M(\sigma_s^2/\sigma_m^2)$.

$$\mathbf{J}_{v1} = \begin{bmatrix} \mathbf{I}_{M-2} & \mathbf{0}_{(M-2)\times 1} & \mathbf{0}_{(M-2)\times 1} & \mathbf{0}_{(M-2)\times(M-1)} \\ \mathbf{0}_{(M-2)\times(M-1)} & \mathbf{0}_{(M-2)\times 1} & \mathbf{I}_{M-2} & \mathbf{0}_{(M-2)\times 1} \end{bmatrix} \tag{24}$$

$$\mathbf{J}_{v2} = \begin{bmatrix} \mathbf{0}_{(M-2)\times 1} & \mathbf{I}_{M-2} & \mathbf{0}_{(M-2)\times 1} & \mathbf{0}_{(M-2)\times(M-1)} \\ \mathbf{0}_{(M-2)\times(M-1)} & \mathbf{0}_{(M-2)\times 1} & \mathbf{0}_{(M-2)\times 1} & \mathbf{I}_{M-2} \end{bmatrix} \tag{25}$$
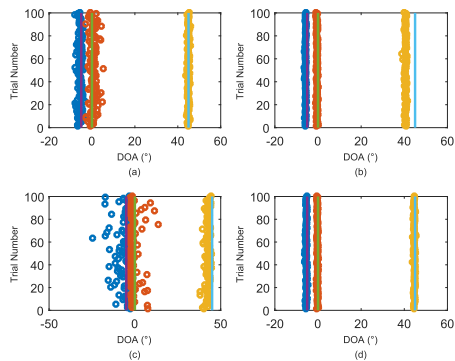
FIGURE 3. The DOA estimation results (SNR = −5dB and L = 500). (a) LRMD [23]. (b) CU-ESPRIT [11]. (c) MCU-ESPRIT. (d) Proposed method (uncorrelated case).

FIGURE 4. The DOA estimation results for uncorrelated sources (SNR = 5dB and L = 500).

Unless stated in the following simulation, it is assumed that the number of far-field sources is $P = 3$. The DOAs of three uncorrelated sources are $\theta_1 = -5°$, $\theta_2 = 0°$ and $\theta_3 = 45°$, respectively, and their phases are set to $\varphi_1 = 10°$, $\varphi_2 = 20°$ and $\varphi_3 = 50°$, respectively. Note that Algorithm 1 is used when sources are uncorrelated and Algorithm 2 is used when sources are coherent. Moreover, the nonuniform noise is $\mathbf{Q} = diag\{20,1,5,7,2,8,1.5,0.5\}$, and $\eta = 100$ is the number of the Monte Carlo trials. The root mean squared error (RMSE) is defined as

$$RMSE = \sqrt{\frac{1}{\eta P} \sum_{i=1}^{\eta} \sum_{p=1}^{P} (\theta_p - \hat{\theta}_{p,i})^2} \qquad (32)$$

where $\hat{\theta}_{p,i}$ is the DOA estimated value of the pth object in the ith trial.

Fig.3 shows the results of DOA estimation achieved by different methods with did 100 trials in this simulation. Among them, the CU-ESPRIT method uses the unitary matrix completion method to eliminate the interference of nonuniform noise. However, the MCU-ESPRIT method does not use it. Also, note that the line in Fig.3 represents the true DOA. It is seen that the noncircular phase has an impact on the CU-ESPRIT method estimation, which has an angular deviation as shown in Fig.3 (b). If the nonuniform noise is not eliminated, the estimated performance will decrease significantly as shown in Fig.3 (c). Although the other methods can estimate correct DOAs, the proposed method has a better estimation performance. In addition, it is worth mentioning that two closely located sources and one source with large angle separation from them are considered in this simulation result, which proves that the proposed method provides higher angular resolution and better estimation performance.

Based on 100 trials, Fig.4 shows ten uncorrelated DOAs estimation of the proposed method, which are $\theta_1 = -40°$, $\theta_2 = -30°$, $\theta_3 = -20°$, $\theta_4 = -10°$, $\theta_5 = 0°$, $\theta_6 = 10°$, $\theta_7 = 20°$, $\theta_8 = 30°$, $\theta_9 = 40°$ and $\theta_{10} = 50°$. It is observed that the proposed method can estimate more sources than sensors because of the fact that the designed virtual
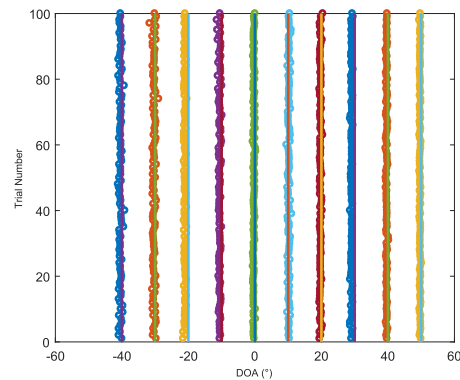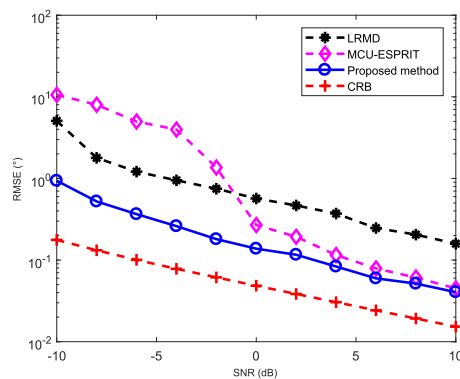

FIGURE 5. The RMSE versus SNRs (L = 500).

array extends the array aperture by utilizing the noncircular property of signals. With theoretical analysis, this method can estimate up to $2M - 2$ uncorrelated sources.

Fig.5 shows the RMSE versus SNRs obtained with different methods and the CRB. It is seen that the LRMD method has better estimation performance than the MCU-ESPRIT method when SNR < 0dB, because the LRMD method eliminates the interference of nonuniform noise. With the increase of SNR, the noise power gradually decreases, and the MCU-ESPRIT method presents better performance by using the extension of the array aperture. Furthermore, the proposed method always maintains performance better than other methods in the entire SNR range.

Fig.6 shows the RMSE versus the number of snapshots obtained with different methods and the CRB. The LRMD method requires a certain number of snapshots to approximately recover the noise-free covariance matrix. Therefore, as seen in Fig.6, the RMSE of the LRMD method is larger than that of the MCU-ESPRIT method when $L \leq 100$. By utilizing the unitary transformation, the proposed method doubles the number of snapshots to achieve excellent performance with a small number of snapshots.

Fig.7 shows the probability of successful detection versus SNRs obtained with different methods. The successful detection satisfies that the absolute error of all estimated angles
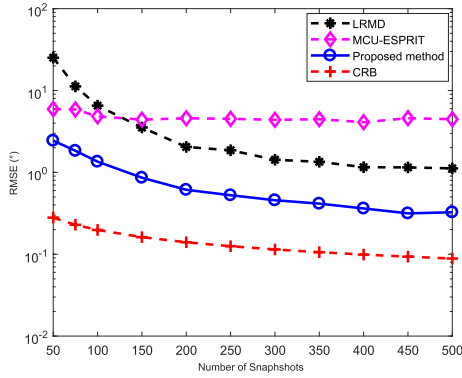
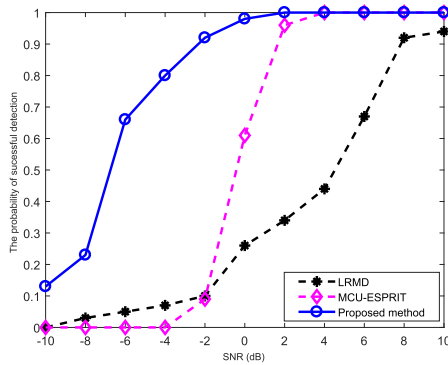**FIGURE 6.** The RMSE versus the number of snapshots (SNR = $-5dB$).

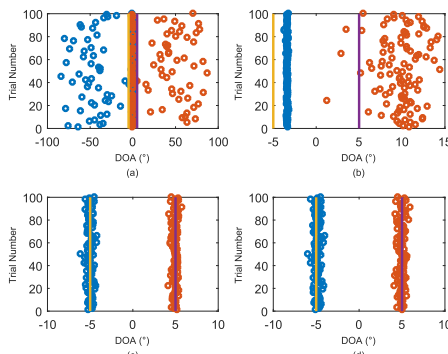**FIGURE 7.** The probability of successful detection versus SNRs ($L = 500$).

FIGURE 8. The DOA estimation results for coherent sources (SNR = 10dB and $L = 64$). (a) LRMD [23]. (b) CU-ESPRIT [11]. (c) MCU-ESPRIT. (d) Proposed method (coherent case).

FIGURE 9. The RMSE for coherent sources versus SNRs ($P = 2$, $\theta_1 = -5°$, $\theta_2 = 5°$ and $L = 64$).

and $\theta_2 = 5°$. The spatial smoothing technique is used in the CU-ESPRIT method, which has $K = 8$ virtual subarrays. Other methods take advantage of the forward-backward spatial smoothing technique, and have $K = 2$ virtual subarrays. The other conditions of this test are the same as in the first one. In addition, it is noteworthy that we use Algorithm 2 of the proposed method in this simulation and the next simulation. As seen in Fig.8, the LRMD method cannot obtain ideal estimation performance when the number of snapshots is small, and the CU-ESPRIT method is affected by the noncircular phase and its estimated performance is also significantly reduced. Since noise powers are small when the SNR is high, the other two methods have similar estimation performance.

Fig.9 shows the RMSE for coherent sources versus SNRs obtained with different methods. Note that these methods have mitigated the coherence of signals. Because the forward-backward spatial smoothing technique reduces the angular resolution, the RMSE of the LRMD method is also very large when the SNR is high. On the other hand, the special structure of the noncircular source was destroyed, which leads to the performance degradation of the proposed method. Fortunately, by extending the array aperture, the proposed method has certain compensation in performance and angular resolution. As seen in Fig.9, using matrix completion technique, there are inevitably some estimation errors, resulting in a slight decline in estimation performance. Therefore, the MCU-ESPRIT method is slightly better than the proposed method when SNR is high.

Fig.10 shows the RMSE versus worst noise power ratios (WNPRs) obtained with different methods, where the WNPR = $\sigma_{max}^2/\sigma_{min}^2$, σ_{max}^2 and σ_{min}^2 denote the maximal and minimal noise power, respectively. As previously assumed, we have $\sigma_{min}^2 = \sigma_8^2 = 0.5$, and σ_1^2 is from 10 to 40. Therefore, the WNPR is varied from 20 to 80. It is seen that both the LRMD method and the proposed method can mitigate the influence of nonuniform noise. However, the proposed method has better performance than the LRMD method.

Fig.11 shows the simulation time comparison between the proposed method and the LRMD method. As mentioned

are smaller than 0.5°. Similar to the previous conclusion, the MCU-ESPRIT method does not achieve successful detection in low SNR region due to the nonuniform noise. The successful detection of the LRMD method is always lower than the proposed method. It is observed that the proposed method has a 100% successfully detection when SNR > 0dB, which further illustrates that the proposed method has superior resolution than other methods.

Fig.8 shows the DOA estimation results for coherent sources with different methods based on 100 trials in this simulation. There are $P = 2$ coherent sources with $\theta_1 = -5°$

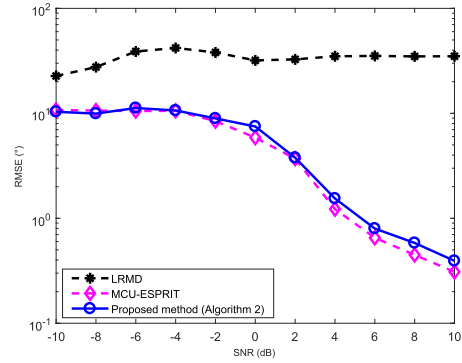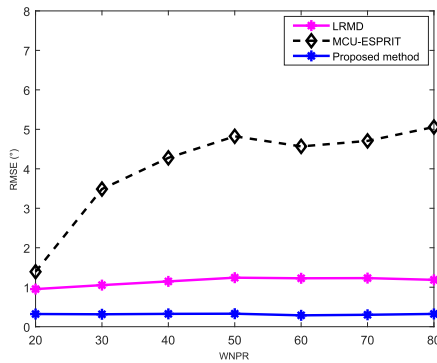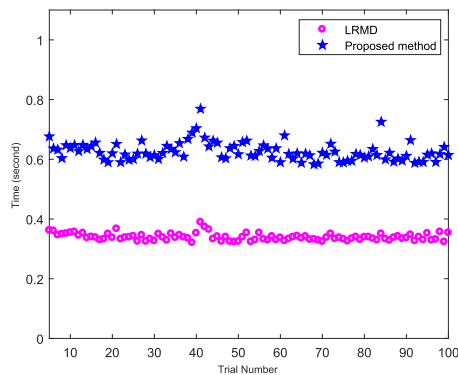**FIGURE 10.** The RMSE versus WNPRs (SNR = −5*dB*, and *L* = 500).

FIGURE 11. The simulation time comparison (SNR = −5*dB*, and *L* = 500).

earlier, the proposed method needs certain computational complexity for the extension of the array aperture. Therefore, the proposed method requires more computation time than the LRMD method. Nevertheless, the proposed method can achieve DOA estimation within one second.

V. CONCLUSION
In this paper, we proposed a unitary matrix completion method to estimate DOAs of noncircular signals in nonuniform noise. The proposed method deals with the virtual array by exploiting the noncircular property of signals. Then, the unitary transformation was utilized to enhance the performance and efficiency of the method. Next, the unitary matrix completion method was applied to mitigate the effect of nonuniform noise with noncircular sources. Finally, the modified CU-ESPRIT algorithm was formulated to estimate the DOAs without the influence of the unknown noncircularity phase. In addition, the estimation problem of coherent noncircular sources was solved by using the forward-backward smoothing technique. The proposed method can effectively suppress the influence of nonuniform noise, and identify more sources than sensors with better estimation performance and higher angular resolution. Simulation results have verified the performances of the proposed method.

REFERENCES
[1] H. Krim and M. Viberg, "Two decades of array signal processing research: The parametric approach," *IEEE Signal Process. Mag.*, vol. 13, no. 4, pp. 67–94, Jul. 1996.

[2] R. O. Schmidt, "Multiple emitter location and signal parameter estimation," *IEEE Trans. Antennas Propag.*, vol. AP-34, no. 3, pp. 276–280, Mar. 1986.

[3] R. Roy and T. Kailath, "Esprit-estimation of signal parameters via rotational invariance techniques," *IEEE Trans. Acoust., Speech, Signal Process.*, vol. 37, no. 7, pp. 984–995, Jul. 1989.

[4] P. Stoica and A. Nehorai, "MUSIC, maximum likelihood and Cramer-Rao bound: Further results and comparisons," in *Proc. IEEE Int. Conf. Acoust., Speech, Signal Process. (ICASSP)*, vol. 4, May 1989, pp. 2605–2608.

[5] H. Huang, J. Yang, H. Huang, Y. Song, and G. Gui, "Deep learning for super-resolution channel estimation and doa estimation based massive MIMO system," *IEEE Trans. Veh. Technol.*, vol. 67, no. 9, pp. 8549–8560, Sep. 2018.

[6] F. Wen, "Computationally efficient DOA estimation algorithm for MIMO radar with imperfect waveforms," *IEEE Commun. Lett.*, to be published. doi: 10.1109/LCOMM.2019.2911285.

[7] A. Zoubir and P. Chargé, Y. Wang, "Non circular sources localization with ESPRIT," in *Proc. 6th Eur. Conf. Wireless Technol. (ECWT)*, Munich, Germany, Oct. 2003, pp. 297–300.

[8] M. Haardt and F. Romer, "Enhancements of unitary ESPRIT for non-circular sources," in *Proc. IEEE Int. Conf. Acoust., Speech, Signal Process. (ICASSP)*, Montreal, QC, Canada, May 2004, p. ii-101.

[9] J. Steinwandt, F. Roemer, M. Haardt, and G. D. Galdo, "R-dimensional esprit-type algorithms for strictly second-order non-circular sources and their performance analysis," *IEEE Trans. Signal Process.*, vol. 62, no. 18, pp. 4824–4838, Sep. 2014.

[10] J. Steinwandt, F. Roemer, M. Haardt, and G. D. Galdo, "Performance analysis of multi-dimensional ESPRIT-type algorithms for arbitrary and strictly non-circular sources with spatial smoothing," *IEEE Trans. Signal Process.*, vol. 65, no. 9, pp. 2262–2276, May 2017.

[11] Z. Liu, J. Wang, and F. Wang, "Conjugate unitary ESPRIT for real sources adapted to the coherent case," *Signal Process.*, vol. 89, no. 7, pp. 1403–1411, Jan. 2009.

[12] L. Yunyi, D. Fei, C. Xiefeng, X. Li, and G. Guan, "Multiple-prespecified-dictionary sparse representation for compressive sensing image reconstruction with nonconvex regularization," *J. Franklin Inst.*, vol. 356, no. 4, pp. 2353–2371, Mar. 2019.

[13] Y. Li, X. Cheng, and G. Gui, "Co-robust-ADMM-net: Joint ADMM framework and DNN for robust sparse composite regularization," *IEEE Access*, vol. 6, pp. 47943–47952, Aug. 2018.

[14] X. Wang, W. Wang, X. Li, Q. Liu, and J. Liu, "Sparsity-aware DOA estimation scheme for noncircular source in MIMO radar," *Sensors*, vol. 16, no. 4, p. 539, Apr. 2016.

[15] X. Yang, G. Li, and Z. Zheng, "DOA estimation of noncircular signal based on sparse representation," *Wireless Pers. Commun.*, vol. 82, no. 4, pp. 2363–2375, 2015.

[16] J. Steinwandt, F. Roemer, and M. Haardt, "Sparsity-based direction-of-arrival estimation for strictly non-circular sources," in *Proc. IEEE Int. Conf. Acoust., Speech, Signal Process. (ICASSP)*, Shanghai, China, Mar. 2016, pp. 3246–3250.

[17] X. Wang, L. Wang, X. Li, and G. Bi, "Nuclear norm minimization framework for DOA estimation in MIMO radar," *Signal Process.*, vol. 135, pp. 147–152, Jun. 2017.

[18] W. Tan, X. Feng, W. Tan, D. Xie, L. Fan, and J. Li, "Direction finding for non-circular sources based on weighted unitary nuclear norm minimization," in *Proc. IEEE Int. Conf. Commun. Technol.*, Chengdu, China, Oct. 2017, pp. 1214–1218.

[19] M. Pesavento and A. B. Gershman, "Maximum-likelihood direction-of-arrival estimation in the presence of unknown nonuniform noise," *IEEE Trans. Signal Process.*, vol. 49, no. 7, pp. 1310–1324, Jul. 2001.

[20] C. E. Chen, F. Lorenzelli, R. E. Hudson, and K. Yao, "Stochastic maximum-likelihood DOA estimation in the presence of unknown nonuniform noise," *IEEE Trans. Signal Process.*, vol. 56, no. 7, pp. 3038–3044, Jul. 2008.

[21] B. Liao, S.-C. Chan, L. Huang, and C. Guo, "Iterative methods for subspace and DOA estimation in nonuniform noise," *IEEE Trans. Signal Process.*, vol. 64, no. 12, pp. 3008–3020, Jun. 2016.

[22] B. Liao, C. Guo, L. Huang, and J. Wen, "Matrix completion based direction-of-arrival estimation in nonuniform noise," in *Proc. IEEE Int. Conf. Digit. Signal Process. (DSP)*, Beijing, China, Oct. 2016, pp. 66–69.

[23] B. Liao, C. Guo, and H. C. So, "Direction-of-arrival estimation in nonuniform noise via low-rank matrix decomposition," in *Proc. IEEE Int. Conf. Digit. Signal Process. (DSP)*, London, U.K., Aug. 2017, pp. 1–4.

[24] K.-C. Huarng and C.-C. Yeh, "A unitary transformation method for angle-of-arrival estimation," *IEEE Trans. Signal Process.*, vol. 39, no. 4, pp. 975–977, Apr. 1991.

[25] M. Haardt and J. A. Nossek, "Unitary ESPRIT: How to obtain increased estimation accuracy with a reduced computational burden," *IEEE Trans. Signal Process.*, vol. 43, no. 5, pp. 1232–1242, May 1995.

[26] Y. Wang, M. Yang, B. Chen, and Z. Xiang, "Improved DOA estimation based on real-valued array covariance using sparse Bayesian learning," *Signal Process.*, vol. 129, pp. 183–189, Dec. 2016.

[27] M. Grant and S. Boyd. (2014). *CVX: Matlab Software for Disciplined Convex Programming, Version 2.1.* [Online]. Available: http://cvxr.com/cvx

[28] M. Lin, L.-L. Cao, J. Ouyang, W. Shi, and K. An, "DOA estimation using virtual array technique for noncirlular signals," in *Proc. IEEE Int. Conf. Wireless Commun. Signal Process. (WCSP)*, Huangshan, China, Oct. 2012, pp. 1–5.

[29] T.-J. Shan, M. Wax, and T. Kailath, "On spatial smoothing for direction-of-arrival estimation of coherent signals," *IEEE Trans. Acoust., Speech, Signal Process.*, vol. ASSP-33, no. 4, pp. 806–811, Apr. 1985.

[30] S. U. Pillai and B. H. Kwon, "Forward/backward spatial smoothing techniques for coherent signal identification," *IEEE Trans. Acoust., Speech Signal Process.*, vol. 37, no. 1, pp. 8–15, Jan. 1989.

[31] Z.-Q. He, Z.-P. Shi, and L. Huang, "Covariance sparsity-aware DOA estimation for nonuniform noise," *Digit. Signal Process.*, vol. 28, pp. 75–81, May 2014.

MENGXING HUANG received the Ph.D. degree from Northwestern Polytechnical University, in 2007. He then joined the Research Institute of Information Technology, Tsinghua University, as a Postdoctoral Researcher. In 2009, he joined Hainan University. He is currently a Professor and a Ph.D. Supervisor of computer science and technology and the Dean of the College of Information and Communication Engineering. He is also the Executive Vice-President of the Hainan Province Institute of Smart City and the Leader of the Service Science and Technology Team, Hainan University. He has published more than 60 academic papers as the first or corresponding author. He has reported 12 patents of invention, owns three software copyrights, and published two monographs and two translations. His current research interests include signal processing for sensor systems, big data, and intelligent information processing. He was awarded one second class and one third class prizes of the Hainan Provincial Scientific and Technological Progress.

JINGJING WANG was born in 1977. She received the Ph.D. degree from Shandong University, in 2012. She visited the University of Pennsylvania, USA, from 2014 to 2015. She is currently a Professor of physics and electronic science with Shandong Normal University. She has published more than 20 papers and applied for five patents. Her research interests include image processing, machine learning, and laser and radar imaging.

XIANPENG WANG was born in 1986. He received the M.S. and Ph.D. degrees from the College of Automation, Harbin Engineering University (HEU), Harbin, China, in 2012 and 2015, respectively. He was a full-time Research Fellow with the School of Electrical and Electronic Engineering, Nanyang Technological University, Singapore, from 2015 to 2016. He is currently a Professor with the College of Information and Communication Engineering, Hainan University. He is the author of over 60 papers published in related journals and international conference proceedings. His major research interests include communication systems, array signal processing, radar signal processing, and compressed sensing and its applications. He has served as a Reviewer for over 20 journals.

LIANGTIAN WAN (M'15) received the B.S. and Ph.D. degrees from the College of Information and Communication Engineering, Harbin Engineering University, Harbin, China, in 2011 and 2015, respectively. From 2015 to 2017, he was a Research Fellow with the School of Electrical and Electronic Engineering, Nanyang Technological University, Singapore. He is currently an Associate Professor with the School of Software, Dalian University of Technology, China. He has published over 40 scientific papers in international journals and conferences. His research interests include social network analysis and mining, big data, array signal processing, wireless sensor networks, and compressive sensing and its application. He is also an Associate Editor of IEEE Access.

YANGHUI ZHU was born in 1994. He received the B.S. degree from Hainan University, Haikou, China, in 2017, where he is currently pursuing the M.S. degree in electronics and communication engineering. His research interests include array signal processing and matrix completion.
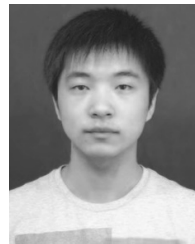
GUOAN BI received the B.Sc. degree in radio communications from the Dalian University of Technology, China, in 1982, and the M.Sc. degree in telecommunication systems and the Ph.D. degree in electronics systems from the University of Essex, U.K., in 1985 and 1988, respectively. Since 1991, he has been with the School of Electrical and Electronic Engineering, Nanyang Technological University, Singapore. His current research interests include DSP algorithms and hardware structures, and signal processing for various applications, including sonar, radar, and communications.

• • •